Chemical Physics Letters 803 (2022) 139851

Contents lists available at ScienceDirect

Chemical Physics Letters

journal homepage: www.elsevier.com/locate/cplett

Conformational diversity of 1-phenylpiperidin-4-one in the gas phase

Alexey V. Eroshin [a], Tran Dinh Phien [b], Peter M. Weber [c], Sergey A. Shlykov [a,*]

[a] Department of Physical and Colloidal Chemistry, Ivanovo State University of Chemistry and Technology, Sheremetevsky Avenue 7, 153000 Ivanovo, Russia
[b] Department of Chemistry and Environment. Vietnam-Russian Tropical Centre. 63 Nguyen Van Huyen, Nghia Do, Cau Giay, Hanoi, Vietnam, Phien Tran
[c] Department of Chemistry, Brown University, Providence R.I. 02912, USA

ARTICLE INFO

Keywords:
Gas electron diffraction
1-phenylpiperidin-4-one
Conformational analysis
Quantum chemical calculations

ABSTRACT

Conformational preferences of substituted, saturated cyclic ketones (piperidones and cyclohexanones) may deviate from those of their oxygenless analogues. 1-Phenylpiperidin-4-one was found to exist in several forms differing by not only position (axial or equatorial) of the aryl-substituent but also by a configuration of the piperidine cycle itself: *chair*-**Eq**, *chair*-**Ax** and *twist* (**Tw**). The ratios of the co-existing species contributions in gas phase predicted by various quantum chemical calculations were confirmed by synchronous gas-phase electron diffraction and mass spectrometric experiments carried out for the vapor at 337 K demonstrating a best fit with the B3LYP-D3/cc-pVTZ combination: **Eq**:**Ax**:**Tw** = 55(13):22(9):23(10) *vs.* 40:35:25.

1. Introduction

Over the last decade, we published results of a series of studies on the structure and conformational properties of 1-X-piperidines in gas phase and solutions [1–7]. In alkylpiperidines, the substituents at the nitrogen atom adopt almost exclusively equatorial (**Eq**) positions relative to the piperidine ring. Less strict 'equatorial rule' concerns the substituents revealing some conjugation involving N atom (phenyl, carbonitrile, alkenyl, etc.). In addition, a peculiar group may be highlighted in which the nitrogen bond configuration is planar or nearly planar (formyl, carbonyl, etc.), so the terms 'equatorial and axial' are not applicable.

In particular, the quantum chemical (QC) and gas-phase electron diffraction (GED) methods applied confirmed an existence of the axial (**Ax**) conformer in gas and liquid states for 1-phenyl- and 1-CN-piperidine, up to ca. 10 and 48 mol.%, respectively [1,2].

Even in the parent compound, piperidine, coexistence of the **Ax** and **Eq** species takes place in the gas-phase equilibrium, see, for example [8,9].

A further search for piperidine derivatives for which a substituent at nitrogen adopts, essentially or even preferably, an axial position brought us to 1-X-piperidin-4-one compounds. DFT and MP2 calculations suggested a noticeable equatorial-to-axial shift when 1-CN-and 1-phenylpiperidine are changed to their −4-one analogues

moreover, this turned out to be relevant for the parent piperidine as well, see data below and in ESI. Later on, it was found that upon 'ketonation' not only a position of a substituent at the N atom changes the preference in positioning relative to the piperidine frame, but, in addition, the six-membered saturated cycle itself tends to inverse to a structure different from a typical chair form. For example, in [10,11] the QC and GED studies of 1,4-cyclohexadione discovered a combination of two types of structures

'chair-equatorial' and 'planar-*twist*'.

In this study, we represent the results of detailed QC and GED/MS studies of the structure and conformational properties of 1-phenylpiperidin-4-one (**1**) along with theoretical predictions for related compounds and of comparisons between piperidine and cyclohexane 1-X derivatives in contrast to their −4-one counterparts. Molecular structures of the **Ax**, **Eq** and twist (**Tw**) conformers of **1** are illustrated in Fig. 1.

1.1. Experimental section

GED/MS. 1 gramm of **1** was purchased from ENAMINE LLC at declared purity of 95 % and then used without further purification.

Synchronous gas-phase electron diffraction and mass spectrometric (GED/MS) experiments for **1** were carried out on the combined EMR100/APDM-1 apparatus described earlier [12–15]. The sample of **1** was loaded into molybdenum effusion cell at atmosphere. Detailed conditions of the GED/MS experiment are listed in Table S1. During all stages of the cell heating, the effusing vapor was continuously monitored by cyclic recording mass spectra each ca. 1.5 min. No noticeable change of the relative ion current was observed throughout the entire experiments. The mass spectra are plotted in Figure S1. The most intensive

* Corresponding author.
E-mail addresses: alexey.yeroshin@gmail.com (A.V. Eroshin), phienhvktqs@gmail.com (T. Dinh Phien), shlykov@isuct.ru (S.A. Shlykov).

https://doi.org/10.1016/j.cplett.2022.139851
Received 2 June 2022; Accepted 4 July 2022
Available online 6 July 2022

peaks correspond to *m/z* 176 $[M]^+$ and 104 $[C_6H_5\text{-}NCH]^+$. Lowering the ionization voltage U_i leads to disappearance of the fragment ions and the only peak is M^+ at $U_i \leq 10$ V that may witness for a single parent of all fragment ions, namely 1-phenyl-1-piperidin-4-one **1**.

Vibrational corrections and starting geometries and vibrational amplitudes for the GED data refinement were derived by the Vibmodule [16] program using a nonlinear relation between Cartesian and internal coordinates on the basis of the B3LYP-D3/cc-pVTZ calculations.

UNEX program package [17] was applied for least-squares procedure of fitting the experimental molecular scattering intensities sM(s), Eq.S1. Convergence of the refinement was based on minimization of the so called agreement factor R_f, Eq. S2. For details of the refinement schemes see **GED analysis** section.

1.2. Computational details

Gaussian09 [18] program was used for the structure optimization and computing of harmonic vibrations. The calculations were performed with use of DFT (B3LYP-D3 with the density functional dispersion correction [19] and M06-2X [20]) and second-order perturbation theory (MP2) combined with 6-311G** and cc-pVTZ basis sets.

A preliminary exploration of possible conformations of **1** was performed by CREST [21,22] program with GFN2-xTB method.

The molecular models were visualized by means of the Chemcraft program [23].

The influence of temperature on the conformer abundance in the gas phase of **1** was assessed by calculating the Gibbs energies with a default option in the Gaussian program at interval 100–1000 K with a step of 100 K using DFT approaches. The potential energy surface (PES) profiles of **1** were scanned for the phenyl group rotation, nitrogen and ring inversions.

2. Results and discussions

2.1. QC structures and conformational preferences

Conformers search. The CREST program localized the following structures

chair forms (two axial (**Ax**) and two equatorial (**Eq**) with different rotational position of the Ph-group each), one *twist* (**Tw**) form, one boat with Ph_{Ax} position and two *twisted-boat* forms.

In the next step, the further search for the conformers, and calculation of their geometric and vibrational parameters were performed by using the Gaussian09 program package.

Of those structures found in the previous step, the following ones (*chair*-**Eq** with orthogonal orientation of the cycles, *twisted-boat* and *boat*) appeared to be not minima but intermediate forms on the PES profiles, see below.

According to DFT calculations, the *chair* conformers with **Ax** and **Eq** positions of the phenyl-substituent as well as the **Tw** form were confirmed to be real minima by DFT and MP2 approaches. Their relative concentrations in the gas phase at 298 K as predicted by different combinations of method/basis set are listed in Table S2. The *chair*-forms balance tends to shift towards the **Ax** conformer in the series B3LYP-D3 → M06-2X → MP2 regardless the basis set, from 1:1 to 2:1.

The **Tw** conformer is predicted to give an essential contribution by DFT methods, up to 22 mol.%, highest by B3LYP-D3/cc-pVTZ, with a favor of the Dunning basis set. At the same time, the MP2 approach manifests for the **Tw** form to be noticeably unfavorable, ~ 3 kcal/mol above the **Ax** form, that corresponds to an abundance of < 1%.

It is worth noting that from DFT the **Tw** conformer is close to the symmetry of C_2 and the fragment C7NC4O is linear, Fig. 1

the fragment at the nitrogen atom NC2C6C7 is flat. On the contrary, the perturbation theory yielded in different arrangement of the latter

it is pyramidal which corresponds, in this case, to the sp^3configuration of the nitrogen atom rather than the sp^2 by DFT.

Selected geometric parameters along with conformer contributions of **1**, derived from quantum chemical calculations with cc-pVTZ basis set and by GED experiment, are compiled in Table 1. A full version of the Table can be found in the ESI, Tables S1-S4.

All the QC calculations converged at a close-to-planar phenyl ring, with deviations not exceeding 1°, and out-of-plane angles for hydrogen atoms within 3° (the largest are for those in the *ortho*-position).

In comparison with the geometry of the oxygen-free analogues, 1-phenylpiperidine [1], there is an increase of the lengths of the C2-C3 and C5-C6 bonds and of dihedral angles and a slight decrease of other bonds and the CNC angle inside the piperidine cycle.

Also, in the case of MP2, the C_s symmetry group is observed for the **Ax** conformer of **1**. As a result, the hydrogen atom in the *ortho*-position of the phenyl ring and the hydrogen bound to the α-carbon atom of the piperidine fragment get closer to each other. The mutual positions of the rings in the case of **Eq** provide a longest distance between the hydrogen atoms in these positions.

One may also note that the piperidine cycle is somewhat large when the phenyl group is attached in the **Ax** position – the intracycle bonds are in general longer by up to 0.015 Å.

As follows from the DFT calculations, the conformer ratios are expected to be substantially affected by temperature. The fraction of **Tw** species increases while the **Eq**:**Ax** ratio is almost unchanged as the temperature raise, see Figure S2.

3. Phenyl-group rotation.

The PES profile of the phenyl group rotation was undertaken in order to estimate the barrier heights. In the case of **Ax**, the rotation is almost barrierless when turning in the range of ca. –25 to + 25° of the φ angle, but it is above 5 kcal/mol to pass through the orthogonal orientation, see Fig. 2. Thus, a C_s symmetry of the equilibrium configuration may also be

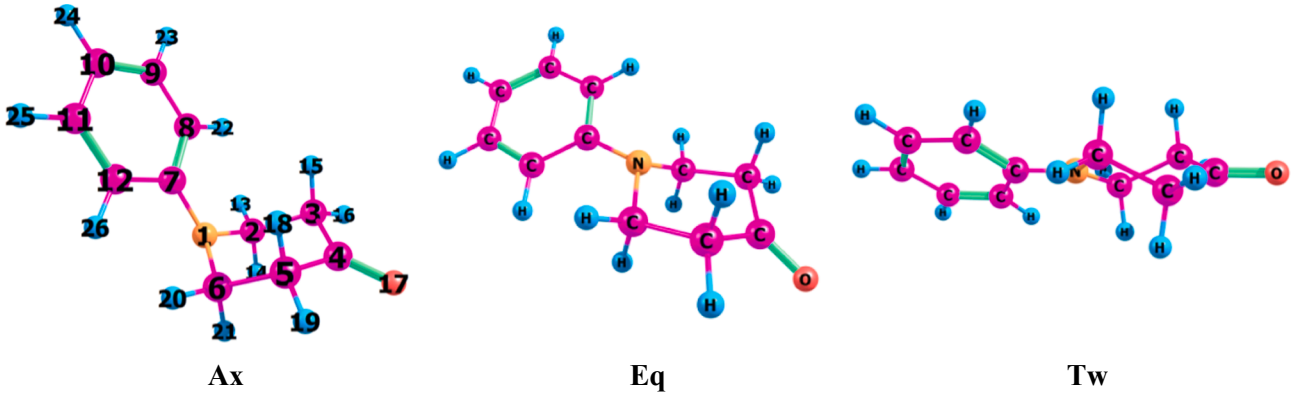

Fig. 1. Molecular models and atoms numbering of the three most favorable conformers of 1-phenylpiperidin-4-one **1**.

Table 1
Selected geometric parameters[a] (Å and degrees), total ΔE and free Gibbs ΔG relative energies (kcal/mol) and contributions X (mol.%) of the conformers of **1**.

	B3LYP-D3/cc-pVTZ			M06-2X/cc-pVTZ			MP2/cc-pVTZ			GED[b]		
	Eq	**Ax**	**Tw**	**Eq**	**Ax**	**Tw**	**Eq**	**Ax**	**Tw**	**Eq**	**Ax**	**Tw**
NC2	1.465	1.455	1.456	1.462	1.453	1.452	1.464	1.456	1.456	1.467(3)	1.457(3)	1.459 (3)
C2C3	1.533	1.547	1.529	1.527	1.540	1.525	1.527	1.539	1.526	1.536(4)	1.550(4)	1.532(4)
C3C4	1.514	1.516	1.515	1.510	1.514	1.512	1.509	1.512	1.510	1.517(4)	1.520(4)	1.518(4)
C4C5	1.514	1.516	1.515	1.510	1.513	1.512	1.509	1.512	1.512	1.517(4)	1.519(4)	1.518(4)
C5C6	1.536	1.546	1.529	1.530	1.539	1.525	1.529	1.539	1.522	1.539(4)	1.550(4)	1.531(4)
C6N	1.456	1.460	1.457	1.452	1.456	1.452	1.453	1.456	1.449	1.458(3)	1.462(3)	1.459(3)
C4O	1.209	1.210	1.207	1.204	1.205	1.203	1.218	1.219	1.216	1.210(5)	1.211(5)	1.209(5)
NC7	1.413	1.405	1.386	1.414	1.417	1.382	1.416	1.405	1.385	1.415(3)	1.407(3)	1.387(3)
C7C8	1.403	1.405	1.408	1.399	1.402	1.404	1.403	1.407	1.407	1.405(3)	1.407(3)	1.410(3)
C7C12	1.399	1.406	1.408	1.394	1.403	1.404	1.400	1.407	1.408	1.401(3)	1.408(3)	1.410(3)
NC2C3	111.1	112.3	111.5	110.8	111.7	110.9	110.5	111.3	111.2	112.2(4)	113.3(4)	111.5[d]
C2C3C4	111.0	110.3	112.5	110.4	109.8	112.0	109.8	109.3	111.5	111.0(11)	110.4(11)	109.7(2)
NC6C5	110.6	111.4	111.5	110.4	111.0	111.0	109.9	111.3	110.1	111.7(4)	112.4(4)	111.5[d]
C6C5C4	111.9	110.7	112.5	111.3	109.9	112.0	110.5	109.3	111.8	111.9(11)	110.8 (11)	110.0(2)
C2NC6	111.9	110.2	118.5	111.5	109.7	119.0	110.7	109.0	118.3	112.9(4)	111.2(4)	118.5[d]
C3C4O	123.0	122.7	123.1	123.0	122.5	123.0	123.1	122.7	123.3	122.6(19)	122.5(19)	120.2(4)
NC2C3C4	53.1	53.1	56.5	54.1	53.9	56.9	55.2	55.6	56.8	51.6(10)	51.7(10)	56.4[d]
NC6C5C4	−52.3	−53.8	56.5	−53.2	−54.9	56.8	−55.1	−55.5	58.9	−50.8(10)	−52.3(10)	57.3[e]
C8C7NC2	−57.6	4.0	17.2	−59.4	11.2	16.8	−62.0	25.1	26.0	−55 (8)	1 (23)	62 (13)
φ[c]	34.9	15.3	16.3	34.8	10.3	14.9	35.6	1.3	15.5	33 (8)[e]	18(23) [e]	56 (13) [e]
Σ(∠CNC)	346.1	349.0	360.0	343.1	346.4	360.0	340.1	343.2	357.6	346.3 [e]	349.2 [e]	355.5 [e]
ΔE + ZPE	0	0.19	1.04	0	0.16	1.08	0.10	0	–			
ΔG_{298}	0	0.09	0.38	0.22	0	0.67	0.39	0	–			
ΔG_{337}	0	0.09	0.31	0.23	0	0.61	–	–	–	–	0.61	0.58
X_{298}, %	42	36	22	34	50	16	34	66	0			
X_{337}, %	40	35	25	33	48	19	–	–	–	55(13)	22(9)	23(10)

[a] equilibrium r_e (QC) and 'geometrically consistent' $r_{h1} = r_a + \Delta r$ (GED) internuclear distances, where r_a is vibrationally averaged distance and Δr is vibrational correction (see Experimental section).

[b] Values in parentheses for the GED data are full errors estimated as $\sigma(r_{h1}) = [\sigma^2_{scale} + (2.5\sigma_{LS})^2]^{½}$, where $\sigma_{scale} = 0.002r$ and σ_{LS} is a standard deviation in least-squares refinement for internuclear distances and as $3\sigma_{LS}$ for angles and vibration amplitudes. For the conformers contribution, a Hamilton criterion [24] was applied to estimate the uncertainty, see Fig. 6. The place-values are such that the last digit of the uncertainty lines up with the last digit of the nominal value.

[c] φ describes the rotational orientation of the phenyl group relative to the piperidine cycle φ = (90 – θ), where θ is an angle C8C7NX X is a dummy atom placed such as the N…X line bisects the C2NC6 valence angle. If φ = 90°, the cycles are orthogonal. The uncertainties for the GED values for φ were adopted as that of C8C7NC2;

[d] fixed parameter;

[e] dependent parameter.

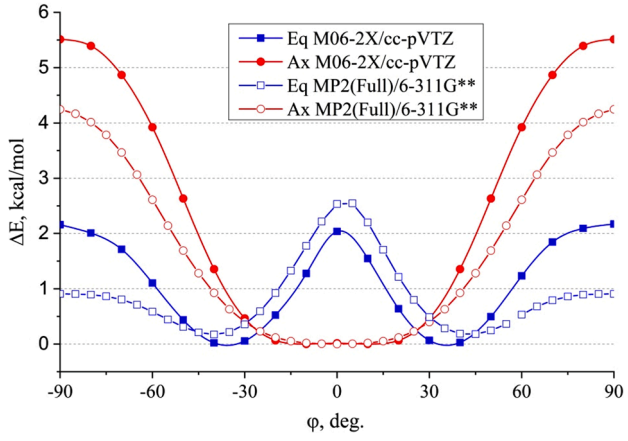

Fig. 2. PES profile of the phenyl group rotation in **Ax** and **Eq** conformers at M06-2X/cc-pVTZ and MP2(Full)/6-311G** levels, see footnotes in Table 1 for the definition of the φ angle.

considered for this conformer. The barriers for **Eq** are approx. 2 kcal/mol for both φ = 0 and 90° orientations. From the MP2 scans, the situation is, in general, the same except the lower barriers near φ = 90°.

The structure of piperidine cycle demonstrates minor distortions from its chair shape throughout the phenyl group rotation.

It is to be noted, that the scans are similar to those for the 'oxygenless' analog, 1-phenyl-piperidine, studied earlier [1].

Nitrogen inversion. This type of the intramolecular inversion to switch between the **Ax** and **Eq** positions of substituents at the nitrogen atom is most energetically preferable for piperidines, as was shown in our earlier papers mentioned in the Introduction section. The nitrogen inversion PES profile for the compound under study **1** was explored by a scan at fixed C7NC4 angle (which is actually an inclination angle of the phenyl group) with a step of 5°, Fig. 3. The barrier is not high and varies from 1.5 to 3.2 kcal/mol, the latter is from the MP2 calculations. Those results are much like those of 1-phenylpiperidine [1].

The structure at C7NC4 angle of ca. 155° was confirmed to represent a transition state (TS) as possessing the only imaginary frequency of 68*i* cm^{-1} (M06-2X/6-311G** with a keyword "TS") the vibrational mode of

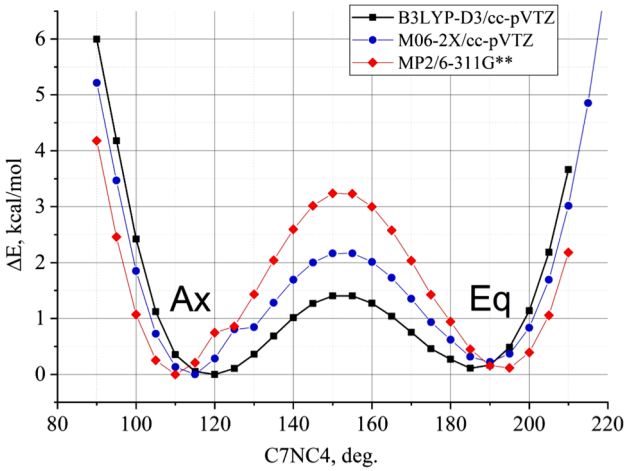

Fig. 3. PES of the nitrogen inversion of **1**.

which tends the TS structure to transform to the **Ax** or **Eq** conformer.

The'unsmooth' range at ca. 110 to 130° derived from M06-2X/cc-pVTZ and MP2/6-311G** combinations is caused by a jump of the phenyl group in the course of the nitrogen inversion when scanning the **Ax** to TS structures because the hydrogens of the two cycles got too close to each other.

Ring inversion. The third conformer, **Tw**, localized in this work for **1** may switch from the **Ax** and **Eq** forms only by another type of inversion – via the piperidine cycle transformation, usually called 'ring inversion'. To find the specific way of the **Eq-Tw-Eq** inversion, the scans by two dihedral angles NC2C3C4 and NC6C5C4 with a step of 10°was performed. A projection of the PES profile is plotted in Fig. 4. The barrier for the **Eq-Tw-Eq** inversion is 4.0 kcal/mol (M06-2X/cc-pVTZ). An attempt to start the ring inversion from the **Ax** form caused an abrupt transformation to the **Eq** conformation before reaching the **Tw** structure.

3.1. GED analysis

Experimental scattering intensities were fitted by theoretical structures refined by least-squares procedure realized within the UNEX program [17].

Vibrational corrections, starting geometries and vibrational amplitudes for the **Ax**, **Eq** and **Tw** conformers were taken from the results of B3LYP-D3/cc-pVTZ calculations, see also the Experimental section for details.

The following parameters (group of parameters) were taken as independent variables to describe the molecular models

(a) r(C-C) in the phenyl group and r(C-N)
(b) r(C-C) in piperidine cycle
(c) r(C-H) and r(C = O)
(d) valence angles in the *chair* piperidine cycle
(e) valence angles in the *twist* piperidine cycle
(f) C-C-H and other angles characterizing the hydrogens position
(g) dihedral angles NC2C3C4, C8C7NC2, C3C2NC6 and C5C6NC2.

Combinations of geometric parameters within a group means that the differences within the group are adopted from the QC calculations and were not refined at the least-squares procedure.

The parameters belonging to the group (f) as well as NC2C3C4 in **Tw**, C3C4(O)C5 (almost planar, i.e. 178-180°) and C2NC7 were fixed.

For the refinement, the vibration amplitudes were combined in 8 groups according to their internuclear distance to the specific bands at the radial distribution (see Fig. 5): 0–1.30, 1.30–1.70, 1.70–2.68, 2.68–3.15, 3.15–3.53, 3.53–4.00, 4.00–4.55, 4.55–10.00 Å;

ratios within the groups were kept equal to the theoretical values.

A sequence of the following stages was applied in the refinement scheme

1) scale factors
2) bond distances (a) and (b)
3) all bond distances, all valence and dihedral angles except fixed ones
4) vibrational amplitudes
5) all mentioned geometric parameters along with the vibrational amplitudes and conformers contributions.

Experimental and theoretical molecular scattering intensities sM(s) and radial distributions f(r) are drawn in Fig. 5 (a) and (b), respectively. Refinement schemes in which only one of the conformers was supposed to contribute to the diffraction patterns were tested, the plotted differences "Exp. – Theor." demonstrate worse fits to the experiment (see colored lines at the bottom of Fig. 5 (b)) than in the case of all three conformers (black line). Moreover, those schemes was tested with fixed quantum chemical structures, see Figure S3.

Refined geometrical parameters and vibrational amplitudes are in good agreement with their theoretical analogs, Table 1 and Table S3. As we noted above, the rotation of the phenyl group in the **Ax** conformer is almost barrierless when turning around the equilibrium orientation in the range of ca. –25 to + 25° (Fig. 2) – this has showed up in a larger, as compared to that of **Eq**, uncertainty in the least-squares refinement, see Table 1.

As for the conformer contributions, in the gas phase **1** the **Tw** form exist in amounts comparable with the **Ax** and **Eq** species – the refinement of the conformers ratio converged at 55(13):22(9):23(3), the given errors are three times least-squares standard deviations. It is worth to mention that the radial distribution functions of theoretical structures from B3LYP-D3/cc-pVTZ approach of **Eq** and **Tw** forms are poorly distinguishable, see Figure S3 which is a complicating factor in the least-squares procedure.

In the next step, the conformer ratio was localized by scanning at fixed contributions with refined structures

the only variables were the scale factors. The steps were taken 10° but 5° closer to the minimum of the agreement factor R_f. The results are plotted in Fig. 6. The region marked in gray corresponds to the error limit estimated by the Hamilton's criterion [24] at 0.05 significance level with a coefficient $R/R_{min} = 1.05$. Since this approach resulted in larger uncertainties than those derived from the structure refinement, we chose the former for the recommended values, i.e. **Eq**

Ax:**Tw** = 55(13)
22(9)
23(10) mol.%.

As was mentioned above, the vibrational corrections as well starting geometric parameters and vibrational amplitudes were taken from the B3LYP-D3/cc-pVTZ calculations. In order to check a reliability of this approach, we also performed a GED data least-squares analysis with the same scheme but using restraints based on the MP2/6-311G** and M06-2X/cc-pVTZ data. The refinement converged at very close geometric and vibrational parameters as well as conformer ratios.

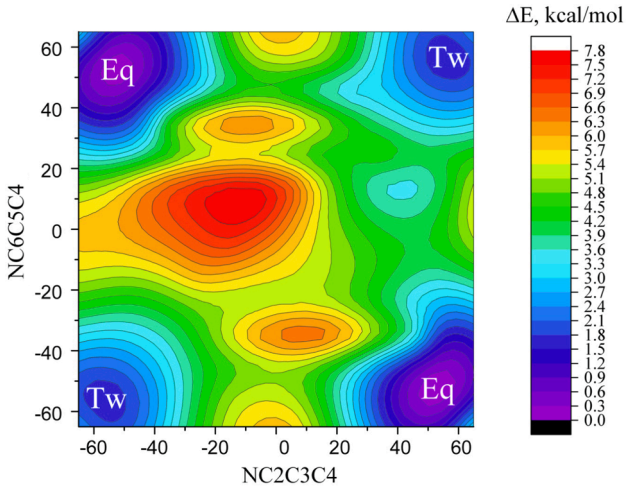

Fig. 4. The projection of the PES profile of the ring inversion of **1** – the relative energy plotted against the dihedral angles NC2C3C4 and NC6C5C4 with a step of 10° by M06-2X/cc-pVTZ.

3.2. Related compounds

A series of QC calculations was performed for other 1-substituted saturated six-membered cycles with and without oxygen atom bound to a carbon atom C4 in order to check a possibility of the twist form to exist in the gas phase as well as an effect of the O-substitution on the axial-equatorial ratio. Results of the calculations at B3LYP-D3/6-311G** level are listed in Table 2.

Introduction of oxygen into the 4th position of 1-X-substituted cyclohexane or piperidine leads to a noticeable stabilization of *chair*-**Ax** relative to *chair*-**Eq** conformer

the B3LYP-D3/6-311G** combination predicts the ratio **Ax**:**Eq** to

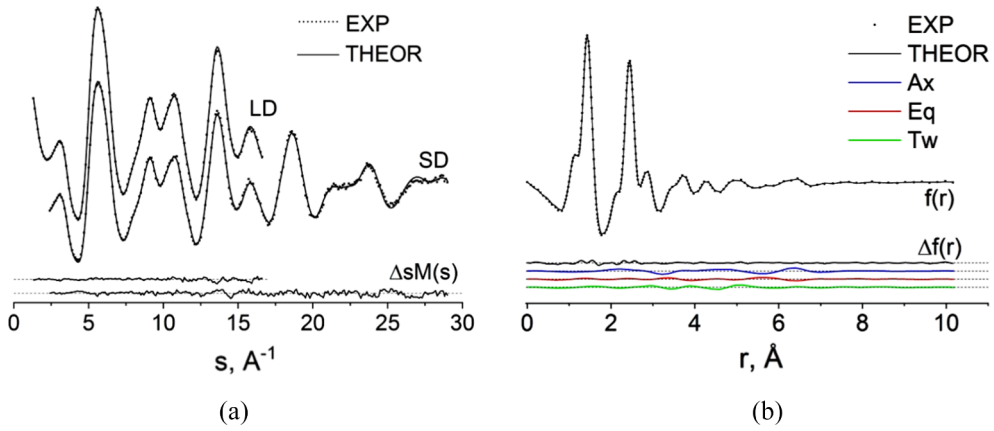

Fig. 5. Experimental and theoretical molecular scattering intensities sM(s) (a) and radial distribution curves f(r) (b). Differences "Exp. – Theor." are given at the bottom for the optimized contributions (black line) as well as for individual conformers (colored lines).

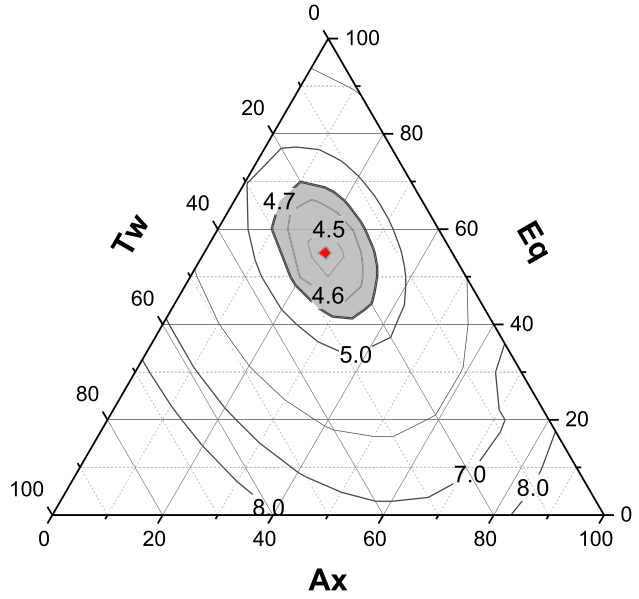

Fig. 6. Agreement factor R_f *vs.* conformers contribution (mol. %), see also text above for details. The red spot corresponds to the minimal R_f = 4.46 %.

increase (in piperidines) from *ca.* 0.7 to 0.9 X = Ph, 0.5 to 1.3 X = CN, 1.4 to 3.7 X = pyridine and (in cyclohexanes) from *ca.* 0.7 to 2.2 X = CN, but not much of change in X-Ph. The latter exists exclusively as a *chair*-**Eq** structure.

The twist form is not inherent for the six-membered cyclic compounds constructed from C and N atoms but in some rare cases like for X = pyridine and phenyl its contribution becomes essential, above 20%, upon 4-oxygen substitution.

A case of doubly oxygen-substituted six-membered cycle was studied in [10] and [11] by QC and GED and resulted in a coexistence of two forms – a *chair* with both planar CC(═O)C fragments and *twist*

the latter is dominating, Table 2.

Different factors, such as the configuration of the carbonyl group and an inclusion of the heteroatoms, are responsible, to that or another extent, for the 'shifts' in the conformational favor. A twist form, a significant contribution of which to the conformational equilibrium appeared to be a sort of a feature of the present work, was also as predicted by theory as well as observed in the experiments for different six-membered cyclic compounds with endo- and *exo*-heteroatoms (O, S, N, etc.), see, for instance, [25–30]. The planarity of the CC(═O)C fragment, in contrast to piramidality of, for example, CS(═O)C group, may

Table 2
Conformational composition at 298 K of the related compounds calculated at B3LYP-D3/6-311G**.

Compound	Equatorial	Axial	Twist
Piperidine	61.8	38.2	0.0
Piperidin-4-one	51.2	48.7	0.1
1-Phenylpiperidine	86.8	12.6	0.6
1-Phenylpiperidin-4-one	41.9	36.2	21.9
Phenylcyclohexane	99.7	0.3	0.0
1-Phenylcyclohexanone-4	98.4	1.1	0.5
CN-cyclohexane	59.8	40.2	0.0
1-CN-cyclohexanone-4	31.5	68.2	0.3
1-CN-piperidine	67.7	32.3	0.0
1-CN-piperidin-4-one	41.1	55.2	3.6
1-Pyridino-piperidine	41.3	58.0	0.6
1-Pyridino-piperidin-4-one	16.2	60.2	23.6
1,4-cyclohexanedione **QC**			
298 K, this work	17 [(a)]		83
435 K, B3LYP/cc-pVTZ[(b)]	38[(a)]		62
GED, 435 K [(b)]	24(10)		76(10)
GED, 383 K [(c)]	30(9)		70(9)

[(a)] – Neither **Eq**, nor **Ax** but a *chair* with both planar CC(═O)C fragments.
[(b)] – Ref. [10].
[(c)] – Ref. [11].

possibly play a crucial role in the twist form stabilization.

4. Conclusions

Analysis of the conformational preferences in the six-membered saturated cyclic compounds in comparison with their ketones revealed a noticeable difference, to a higher extent for piperidines rather than cyclohexanes. Most notable are the cases of 1-X-piperidin-4-one derivatives with the substituents X = Ph, CN or Py, due probably to peculiarities of their interaction with the nitrogen lone pair. The *chair*-axial conformer becomes more stable and may even dominate over the *chair*-equatorial form. Moreover, a *twist* structure of the cycle (piperidine or cyclohexane) appears in the keto-derivatives.

The ratios of the co-existing species contributions in the gas phase of **1** predicted by various quantum chemical calculations were confirmed by GED/MS and are in good agreement with the B3LYP-D3/cc-pVTZ combination

Eq:**Ax**:**Tw** = 55(13):22(9):23(10) *vs.* 40:35:25. The MP2 and M06-2X approaches overestimate the abundance of the Ax form by 2 to 3 times.

The nitrogen atom bond configuration in **1**, see the line marked as Σ(∠CNC) in Table 1, shows a pyramidality increasing by approx. 3° from **Ax** to **Eq**. On the other hand, the sum of the valence angles at N in the *twist* form is very close to 360° witnessing for sp^2 hybridization unlike

the sp^3 in the *chairs*. The MP2 method predicts it to be slightly pyramidal, 357° and it is to be noted that the GED analysis with the B3LYP-D3/cc-pVTZ restraints (see above) converged, nevertheless, at 355.5°.

Funding

S.A.S. is grateful to the Ministry of Science and Higher Education of the Russian Federation, grant FZZW-2020–0007. P.M.W. acknowledges funding by the U.S. Department of Energy, Office of Science, Basic Energy Sciences, Award # DE-SC0017995, and the National Science Foundation, Award # CHE-1953839.

CRediT authorship contribution statement

Alexey V. Eroshin: Investigation, Writing – original draft, Project administration. **Tran Dinh Phien:** Investigation. **Peter M. Weber:** Writing – original draft. **Sergey A. Shlykov:** Conceptualization, Methodology, Writing – original draft, Writing – review & editing.

Declaration of Competing Interest

The authors declare that they have no known competing financial interests or personal relationships that could have appeared to influence the work reported in this paper.

Acknowledgements:

The gas-phase electron diffraction/mass-spectrometric experiments were carried out using the GED/MS equipment (https:// www.isuct.ru/department/ckp/structure/ged-ms) of the resources of the Center for Shared Use of Scientific Equipment of the ISUCT (with the support of the Ministry of Science and Higher Education of the Russian Federtion, grant No. 075-15-2021-671).

Appendix A. Supplementary material

Supplementary data to this article can be found online at https://doi.org/10.1016/j.cplett.2022.139851.

References

[1] S.A. Shlykov, T.D. Phien, Y. Gao, P.M. Weber, Structure and conformational behavior of N-phenylpiperidine studied by gas-phase electron diffraction and quantum chemical calculations, J. Mol. Struct. 1132 (2017) 3–10, https://doi.org/10.1016/j.molstruc.2016.06.048.
[2] S.A. Shlykov, T.D. Phien, P.M. Weber, Intramolecular inversions, structure and conformational behavior of gaseous and liquid N-cyanopiperidine. Comparison with other 1-cyanoheterocyclohexanes, J. Mol. Struct. 1138 (2017) 41–49. https://doi.org/10.1016/j.molstruc.2017.03.006.
[3] S.A. Shlykov, T.D. Phien, Y. Gao, P.M. Weber, Molecular structure and conformational properties of N-cyclohexylpiperidine as studied by gas-phase electron diffraction, mass spectrometry, IR spectroscopy and quantum chemical calculations, Struct. Chem. 26 (2015) 1501–1512, https://doi.org/10.1007/s11224-015-0602-z.
[4] T.D. Phien, S.A. Shlykov, N-substituted akyl- and nonalkylpiperidines equatorial, axial or intermediate conformations?, comput, Theor. Chem. 1087 (2016) 26–35, https://doi.org/10.1016/j.comptc.2016.04.025.
[5] T.D. Phien, S.A. Shlykov, P.M. Weber, The influence of steric and orbital intereactions on molecular structure in N-substituted piperidines, Izv. Vyss. Uchebn. Zaved. Khim Khim. Tekhnol. 59 (2016) 19–26, https://doi.org/10.6060/tcct.20165911.5464.
[6] T.D. Phien, S.A. Shlykov, B.A. Shainyan, Molecular structure and conformational behavior of 1-methyl-1-phenylsilacyclohexane studied by gas electron diffraction, IR spectroscopy and quantum chemical calculations, Tetrahedron. 73 (2017) 1127–1134, https://doi.org/10.1016/j.tet.2017.01.008.
[7] S.A. Shlykov, T.D. Phien, N.H. Trang, Orbital interaction between electron lone pair and carbonyl group in N-trifluoroacetylpiperidine and N-piperidine amides planar and non-planar nitrogen bond configurations, Tetrahedron. 73 (35) (2017) 5311–5320.
[8] G. Gundersen, D.W.H. Rankin, The Gas-phase Molecular Structure of Piperidine Studied by Electron Diffraction., Acta Chem. Scand. 37a (1983) 865–874. https://doi.org/10.3891/acta.chem.scand.37a-0865.
[9] J.E. Parkin, P.J. Buckley, C.C. Costain, The microwave spectrum of piperidine equatorial and axial ground states, J. Mol. Spectrosc. 89 (1981) 465–483, https://doi.org/10.1016/0022-2852(81)90040-0.
[10] M. Frogner, R.D. Johnson, L. Hedberg, K. Hedberg, 1,4-cyclohexanedione. composition, molecular structures, and internal dynamics of the vapour an electron diffraction investigation augmented by molecular orbital calculations, J. Phys. Chem. A 117 (43) (2013) 11101–11106.
[11] Q. Shen, S. Samdal, The molecular structures and conformational compositions of 1,3 cyclohexanedione and 1,4 cyclohexanedione as determined by gas-phase electron diffraction and theoretical calculation, J. Mol. Struct. 1005 (2011) 156–160, https://doi.org/10.1016/j.molstruc.2011.08.043.
[12] G.V. Girichev, A.N. Utkin, Y.F. Revichev, Modernization of the EMR-100 setup for the studies of gases, Prib. Tekh. Eksp. (1984) 187–190.
[13] G.V. Girichev, S.A. Shlykov, Y.F. Revichev, Apparatus for studies of the molecular structures of non-saturated compounds, Prib. Tekh. Eksp. 167–169 (1986).
[14] S.A. Shlykov, G.V. Girichev, A radiofrequency mass spectrometer based on APDM-1 unit for the mass range of 1–1600 amu, Prib. Tekh. Eksp. 141–142 (1988).
[15] G.V. Girichev, S.A. Shlykov, V.N. Petrova, N.Y. Subbotyina, S.B. Lapshina, T. G. Danilova, Equipment and technique of joint gas electron diffraction and mass spectrometric experiment and their application to the study of titanium trihalide molecules, Izv. Vyss. Uchebn. Zaved. Khim Khim. Tekhnol. 31 (1988) 46–49.
[16] Y.V. Vishnevskiy, Y.A. Zhabanov, New implementation of the first-order perturbation theory for calculation of interatomic vibrational amplitudes and corrections in gas electron diffraction, J. Phys. Conf. Ser. 633 (2015) 012076.
[17] Y.V. Vishnevskiy, UNEX version 1 (2022) 6.
[18] M.J. Frisch, G.W. Trucks, H.B. Schlegel, G.E. Scuseria, M.A. Robb, J.R. Cheeseman, G. Scalmani, V. Barone, B. Mennucci, G.A. Petersson, H. Nakatsuji, M. Caricato, X. Li, H.P. Hratchian, A.F. Izmaylov, J. Bloino, G. Zheng, J.L. Sonnenberg, M. Hada, M. Ehara, K. Toyota, R. Fukuda, J. Hasegawa, M. Ishida, T. Nakajima, Y. Honda, O. Kitao, H. Nakai, T. Vreven, J.A. Montgomery, J.E. Peralta, F. Ogliaro, M. Bearpark, J.J. Heyd, E. Brothers, K.N. Kudin, V.N. Staroverov, R. Kobayashi, J. Normand, K. Raghavachari, A. Rendell, J.C. Burant, S.S. Iyengar, J. Tomasi, M. Cossi, N. Rega, J. M. Millam, M. Klene, J.E. Knox, J.B. Cross, V. Bakken, C. Adamo, J. Jaramillo, R. Gomperts, R.E. Stratmann, O. Yazyev, A.J. Austin, R. Cammi, C. Pomelli, J.W. Ochterski, R.L. Martin, K. Morokuma, V.G. Zakrzewski, G.A. Voth, P. Salvador, J.J. Dannenberg, S. Dapprich, A.D. Daniels, Ö. Farkas, J.B. Foresman, J. V Ortiz, J. Cioslowski, D.J. Fox, J.A. Montgomery Jr., Gaussian 09, Rev A.1, Gaussian Inc Wallingford CT. (2009).
[19] S. Grimme, J. Antony, S. Ehrlich, H. Krieg, A consistent and accurate ab initio parametrization of density functional dispersion correction (DFT-D) for the 94 elements H-Pu, J. Chem. Phys. 132 (15) (2010) 154104.
[20] Y. Zhao, N.E. Schultz, D.G. Truhlar, Design of density functionals by combining the method of constraint satisfaction with parametrization for thermochemistry, thermochemical kinetics, and noncovalent interactions, J. Chem. Theory Comput. 2 (2006) 364–382, https://doi.org/10.1021/ct0502763.
[21] P. Pracht, F. Bohle, S. Grimme, Automated exploration of the low-energy chemical space with fast quantum chemical methods, Phys. Chem. Chem. Phys. 22 (2020) 7169–7192, https://doi.org/10.1039/C9CP06869D.
[22] S. Grimme, Exploration of chemical compound, conformer, and reaction space with meta-dynamics simulations based on tight-binding quantum chemical calculations, J. Chem. Theory Comput. 15 (2019) 2847–2862, https://doi.org/10.1021/acs.jctc.9b00143.
[23] G.A. Zhurko, D.A. Zhurko, ChemCraft version 1.6 (build 312) http://www.chemcraftprog.Com/Index.Html. (n.d.).
[24] W.C. Hamilton, Significance tests on the crystallographic R factor, Acta Crystallogr. 18 (1965) 502–510, https://doi.org/10.1107/S0365110X65001081.
[25] F. Freeman, B.A. Shainyan, Relative energies of conformations and sulfinyl oxygen-induced pentacoordination at silicon in 4-bromo- and 4,4-dibromo-4-silathiacyclohexane 1-oxide a computational study, Int. J. Quantum Chem. 105 (2005) 313–324, https://doi.org/10.1002/qua.20707.
[26] F. Freeman, N. Asgari, B. Entezam, F. Gomarooni, J. Mac, M.H. Nguyen, N.N. T. Nguyen, T.P. Nguyen, N.B. Pham, P. Sultana, T.S. Welch, B.A. Shainyan, Computational study of sulfoxides of thiacyclohexane, 4-silathiacyclohexane, 4-fluoro-4-silathiacyclohexane, and 4,4-difluoro-4-silathiacyclohexane relative energies of conformations and sulfinyl oxygen stabilized pentacoordinate silicon in boat and twis, Int. J. Quantum Chem. 101 (2005) 40–54, https://doi.org/10.1002/qua.20176.
[27] B.A. Shainyan, Computational study of 4-fluoro-4-chloro- and 4-fluoro-4-bromo-4-silathiacyclohexane S-oxides effect of halogen on the S□O→Si intramolecular coordination in the boat and twist conformers, Int. J. Quantum Chem. 107 (2007) 189–199, https://doi.org/10.1002/qua.21051.
[28] S.A. Shlykov, N.I. Giricheva, G.N. Eyler, H. Oberhammer, Gas-phase structure and conformational properties of 3,3,6,6-tetramethyl-1,2,4,5-tetroxane, J. Phys. Chem. A. 111 (2007) 1368–1373, https://doi.org/10.1021/jp067763e.
[29] I. Yavari, M. Haghdadi, R. Amiri, AB initio molecular orbital study of 1,2-dithiane and 1,2,4,5-tetrathiane, Phosphorus. Sulfur. Silicon Relat. Elem. 179 (2004) 2015–2023, https://doi.org/10.1080/10426500490473537.
[30] C.H. Bushweller, J. Golini, G.U. Rao, J.W. O'Neil, Conformational analysis in multisulfur heterocycles. V. Activation parameters for the chair.dbr. twist equilibration in duplodithioacetone by direct thermal stereomutation and total nuclear magnetic resonance line shape analysis, J. Am. Chem. Soc. 92 (1970) 3055–3058, https://doi.org/10.1021/ja00713a023.